# Interactions between Heme Proteins and Dextran Sulfate in Layer-by-Layer Assembly Films

**Pingli He and Naifei Hu***

*Department of Chemistry, Beijing Normal University, Beijing 100875, People's Republic of China*

*Received: January 1, 2004; In Final Form: April 30, 2004*

The protein hemoglobin (Hb) or myoglobin (Mb) in a variety of net surface charge states at different pH values was alternately assembled with negatively charged polysaccharide dextran sulfate (Dex) into layer-by-layer (LBL) films on solid surfaces. The proteins in the LBL $\{Dex/protein\}_n$ films demonstrated a pair of well-defined cyclic voltammetric (CV) peaks at about −0.35 V vs SCE at pH 7.0 for the heme Fe(III)/Fe(II) redox couple at pyrolytic graphite electrodes, and a sensitive Soret spectroscopic absorption band at around 410 nm on quartz slides. Quartz crystal microbalance (QCM), CV, and UV−vis spectroscopy were then used to characterize the $\{Dex/protein\}_n$ films. The interaction between the proteins and Dex under different conditions was investigated, and the driving forces for the LBL $\{Dex/protein\}_n$ film assembly were explored. The factors influencing the protein adsorption on the Dex layer surface, such as the concentration of proteins, the ionic strength of protein solutions, and the applied electric field, were also studied in detail. The results suggest that electrostatic interaction is the most important driving force for the film assembly. Even when the proteins had net negative charges on their surface the localized Coulombic attraction between the positively charged surface groups of the proteins and the negatively charged Dex surface would lead to a stable film assembly, although the amount of adsorbed proteins in this case was less than that when the proteins had net positive charges on their surface.

## 1. Introduction

Surface modification by deposition of ordered protein films constitutes one of the major objectives of biochemistry and biotechnology. Such a nanoconstruction of proteins also creates a novel frontier domain between materials and life sciences. Thus, spatially organized protein layers within supramolecular aggregates play a significant role in biologically related studies.[1,2] In this respect, a novel concept of layer-by-layer (LBL) assembly has recently been developed for fabricating multilayers by alternate adsorption of oppositely charged proteins and polyelectrolytes or nanoparticles.[3,4] The advantage of the LBL method is that the layer composition and thickness can be precisely tailored by varying the type of charged species and the number of adsorption cycles according to a predesigned architecture. The LBL technology is also quite simple for film assembly, especially compared to the Langmuir−Blodgett method. The protein LBL films have been used in various biologically related applications such as enzyme-catalyzed synthesis,[5] biosensors,[6] and gene delivery.[7] Particularly, direct electron exchange between redox proteins and underlying electrodes has been realized recently in LBL protein films.[8,9] Direct electrochemistry of redox proteins or enzymes in LBL films can establish a working model for the fundamental studies of electron transfer between enzymes in biological systems, and provide a foundation for fabricating a new type of biosensors, bioreactors, and biomedical devices without using mediators.[10,11] These LBL protein films exhibit electrochemical properties similar to those of cast protein films,[12] but provide nanometer-scale thickness control and better stability.

The controlled incorporation of proteins in LBL films first requires understanding of the protein adsorption mechanism. The main driving force or major stabilizing interaction in alternate LBL film assembly is usually thought to be electrostatic attraction between oppositely charged species.[13] However, the actual situation is more complicated when proteins are involved. While in most cases the net surface charges of proteins and the overall charges of polyions or nanoparticles were opposite in LBL assembly, in some cases when the proteins and polyelectrolytes or nanoparticles carried the same overall charges a considerable amount of adsorption of the proteins on the surface of polyions or nanoparticles was also observed. Until now, only a few studies have been devoted to this "counterintuitive" phenomenon. Ladam et al.[14−16] investigated the interactions between proteins and polyelectrolytes of different types and with different surface charges by means of scanning angle reflectometry (SAR). They found that the proteins strongly interacted with the polyelectrolytes regardless of their overall charges. While the net surface charges of the protein were (for example) negative, the protein might still have positive patches on its surface which allowed localized binding of the protein to a negatively charged surface. Schenkman et al.[17] found that cytochrome P450 enzymes could be adsorbed on both positively and negatively charged polyion layers as a consequence of differently signed charge patches on different sides of the enzymes. In our recent study,[18] LBL films of heme proteins and $SiO_2$ nanoparticles were constructed on various solid substrates under different conditions. We found that, even when the proteins and silica were both negatively charged, stable LBL films of proteins and $SiO_2$ nanoparticles were successfully fabricated, suggesting the importance of localized Coulombic attractions between the negatively charged nanoparticle surface

* To whom correspondence should be addressed. E-mail: hunaifei@bnu.edu.cn.

10.1021/jp049974u CCC: $27.50 
Published on Web 08/10/2004

**SCHEME 1: Chemical Structure of Dextran Sulfate**

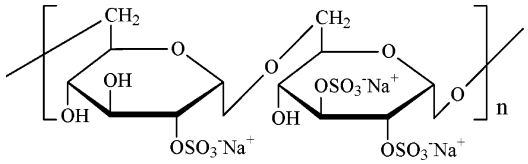


and positively charged amino acid residues on the protein surfaces in the assembly. Moreover, other driving forces such as hydrogen bonding and hydrophobic attraction may also play an important role in some cases, as recognized in polymer−polymer LBL assembly.[19−21] However, to the best of our knowledge, little systematic study on the nature of interaction or driving forces in LBL assembly of proteins and polyelectrolyte has been reported up to now. The understanding of the interaction not only will be of significance for the design of new protein multilayer architectures, but also will allow one to gain further insight into the role of surface charges in protein adsorption processes.

As biodegradable and environmentally benign materials, polysaccharides have been extensively used in medical and pharmaceutical areas, among others.[22] Therefore, it would be advantageous to use biocompatible polysaccharides instead of synthetic polymers as film-forming materials for fabricating protein LBL nanostructures. Dextran sulfate (Dex) is one commonly used polysaccharide that has a lot of negative charges on its backbone. The chemical structure of Dex is shown in Scheme 1. Dex has been used to assemble LBL films with positively charged polyions such as chitosan.[23−25]

In the present paper, the interaction between Dex and some heme proteins in LBL assembly was investigated in a systematic way. We selected hemoglobin (Hb) and myoglobin (Mb) as model proteins because they have sensitive spectroscopic absorption, good electroactivity, and different net surface charges at different pH values. The LBL films of Dex and heme proteins on various solid surfaces under different conditions were characterized by UV−vis spectroscopy, quartz crystal microbalance (QCM), and cyclic voltammetry (CV). Various influencing factors on the protein adsorption, such as the concentration of proteins, the ionic strength, and the applied electric field, were also discussed.

## 2. Experimental Section

**2.1. Chemicals.** Bovine hemoglobin (Hb, MW 66 000), horse heart myoglobin (Mb, MW 17800), and dextran sulfate (Dex, MW 500 000) were from Sigma and used as received. Poly(ethylene imine) (PEI, 90%, MW 60 000) and 3-mercapto-1-propanesulfonate (MPS, 90%) were from Aldrich. Buffers were 0.1 M acetate (pH 5), 0.05 M sodium dihydrogen phosphate (pH 7), or 0.05 M boric acid (pH 9), all containing 0.1 M KBr. Buffer pHs were adjusted to the desired values with 0.1 M HCl or KOH solutions. All other chemicals were of reagent grade. Water was purified by successive ion exchange and distillation.

**2.2. Assembly of Layer-by-Layer Films.** For electrochemical study, basal plane pyrolytic graphite (PG, Advanced Ceramics, geometric area 0.16 $cm^2$) disk electrodes were polished on a metallographic sandpaper of 400 grit while being flushed with water. The electrodes were then ultrasonicated in pure water for 30 s and dried in air. A precursor monolayer of positively charged PEI was adsorbed by immersing the PG electrodes into PEI solutions (3 mg $mL^{-1}$) for 20 min. After being washed in pure water, the PG/PEI electrodes were alternately immersed for 20 min in Dex solutions (3 mg $mL^{-1}$) and aqueous Hb or Mb solutions (1 mg $mL^{-1}$) with intermediate water washing and nitrogen stream drying. This cycle was repeated to obtain the desired number of layers.

For UV−vis spectroscopic study, a quartz slide (1 × 4 cm, 1 mm thick) was treated by immersing it in a freshly prepared "piranha" solution (3:7 volume ratio of 30% $H_2O_2$ and 98% $H_2SO_4$) for 20 min, rinsing it carefully with water, and then drying it with a nitrogen stream. (**Caution:** Piranha solution should be handled with extreme care, and only small volumes should be prepared at any time.) The slide with negative charges on the surface was then immersed into PEI solution for 20 min to adsorb PEI and make the slide surface become positively charged. The following procedure to fabricate LBL $\{Dex/protein\}_n$ films on the quartz slide/PEI surface was the same as on PG electrodes. The Soret absorption band of heme proteins was used to monitor the growth of assembly of the LBL $\{Dex/protein\}_n$ films by UV−vis spectroscopy.

For quartz crystal microbalance (QCM) study, the AT-cut quartz resonators were coated by gold thin film electrodes (area 0.196 $cm^2$) on both sides, and their fundamental resonant frequency was 8 MHz. Gold resonator electrodes were first soaked in a freshly prepared piranha solution for 10 min, and then washed in water and pure ethanol successively. The freshly cleaned gold QCM electrode was then immersed in an MPS ethanol solution (4 mM) for 24 h to form an MPS monolayer and introduce negative charges on the gold surface. The precursor layer of PEI and following LBL $\{Dex/protein\}_n$ films were then assembled on the Au/MPS surface as on the PG electrodes. After each adsorption step, the Au resonator electrode was washed in pure water for 1 min, dried in a nitrogen stream, and then measured by QCM.

**2.3. Apparatus and Procedures.** A CHI 420 electrochemical workstation (CH Instruments) was used for CV and QCM studies. For electrochemical studies, a conventional three-electrode cell was used with a saturated calomel electrode (SCE) as the reference electrode, a platinum wire was used as the counter electrode, and a PG disk modified with films was used as the working electrode. CVs at protein film electrodes were performed in buffers containing no protein. Buffers were purged with highly purified nitrogen for at least 10 min prior to a series of experiments. A nitrogen environment was then kept in the cell by continuously bubbling $N_2$ during the whole experiment. A Cintra 10e UV−visible spectrophotometer (GBC) was used for UV−vis spectroscopy. All experiments were done at ambient temperature of 20 ± 2 °C.

## 3. Results

**3.1. Fabrication of Layer-by-Layer $\{Dex/Protein\}_n$ Films by Regular Growth Mode.** Dex is a negatively charged polysaccharide in solution, while Hb and Mb, with their isoelectric point at pH 7.0−7.4 [26,27] and 6.8−7.0,[3,28] respectively, have considerable positive surface charges at pH 5.0. Thus, LBL films of Dex and the heme proteins at pH 5.0 were successfully assembled on different substrates by Coulombic attraction between them. These regularly grown films are designated as $\{Dex/protein\ (pH\ 5.0)\}_n$, where $n$ is the number of bilayer adsorption cycles.

Both Hb and Mb have a strong Soret absorption band for their heme groups at about 410 nm,[29] and UV−vis spectroscopy was used to monitor the growth of LBL $\{Dex/protein(pH\ 5.0)\}_n$ films on quartz slides with a precursor of PEI on the surface. Taking Hb as an example, the UV−vis spectra at consecutive cycles of the adsorption of Dex/Hb bilayer on a quartz slide

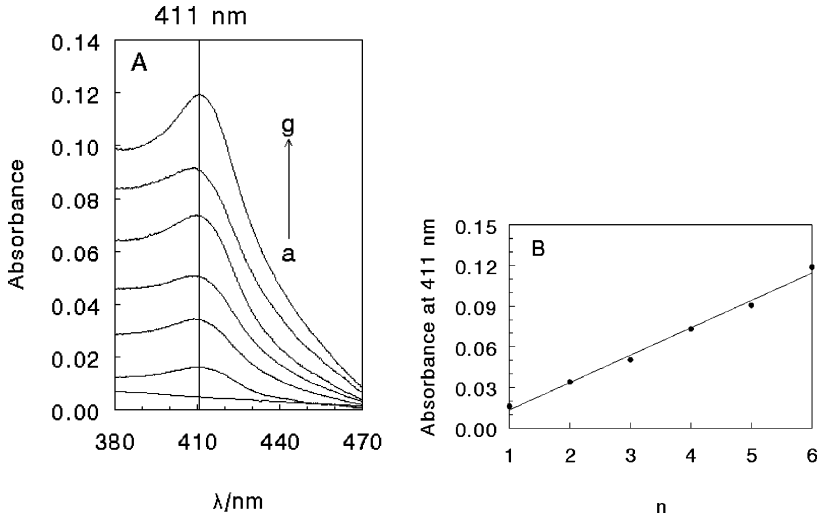


**Figure 1.** (A) UV−vis spectra on quartz slides for (a) PEI/Dex bilayer and (b)−(g) LBL PEI/{Dex/Hb(pH 5.0)}$_n$ films with different numbers of bilayers ($n$); (b)−(g), $n = 1-6$. (B) Dependence of absorption at 411 nm of PEI/{Dex/Hb(pH 5.0)}$_n$ films on number of bilayers ($n$).

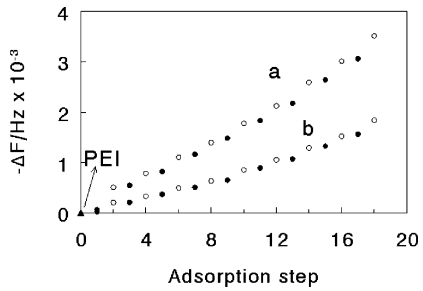


**Figure 2.** Shift of QCM frequency with alternate adsorption steps for (a) {Dex/Hb(pH 5.0)}$_n$ and (b) {Dex/Hb(pH 9.0)}$_n$ films on the Au/MPS/PEI surface: (●) Dex adsorption steps; (○) Hb adsorption steps.

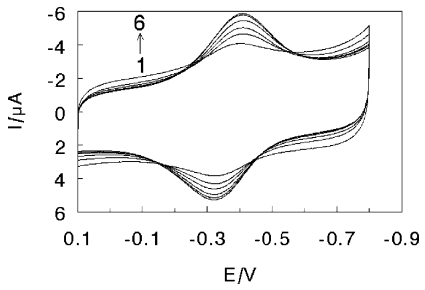


**Figure 3.** Cyclic voltammograms of LBL {Dex/Mb(pH 5.0)}$_n$ films at scan rate of 0.2 V s$^{-1}$ in pH 7.0 buffer solutions with different numbers of bilayers.

showed that the Soret absorption band at 411 nm increased linearly with the number of bilayers with a correlation coefficient of 0.997 (Figure 1). This confirms that the multibilayer {Dex/Hb(pH 5.0)}$_n$ films are built up in a regular and reproducible fashion, and the amount of Hb adsorbed in each bilayer is nearly the same.

QCM was also used to monitor the assembly of LBL {Dex/protein(pH 5.0)}$_n$ films. Based on Sauerbrey equation,[30] the following relationship is obtained between adsorption mass, $\Delta M$ (g), and frequency shift, $\Delta F$ (Hz), by taking into account the properties of quartz resonator used in this work:

$$\Delta F = -7.40 \times 10^8 \Delta M \quad (1)$$

Thus, 1 Hz of frequency decrease corresponds to 1.35 ng of mass increase. QCM data were also used to estimate the nominal thickness of adsorbed layer for {Dex/protein(pH 5.0)}$_n$ films, assuming each layer is arranged compactly. The thickness, $d$ (cm), can be expressed by

$$d = -3.4 \times 10^{-9} \Delta F/\rho \quad (2)$$

where $\rho$ is the density of the film material (g cm$^{-3}$).

For instance, QCM results for {Dex/Hb(pH 5.0)}$_n$ films grown on Au/MPS/PEI surface showed a roughly linear decrease of frequency with the adsorption step (Figure 2a), indicating the building up of {Dex/Hb(pH 5.0)}$_n$ films is in a regular or linear manner, by which the amount of Dex and Hb adsorbed in each cycle was almost the same, respectively. If the density of Dex film was assumed to be $1.2 \pm 0.1$ g cm$^{-3}$,[31] the average frequency decrease of $54 \pm 15$ Hz for each Dex adsorption layer would correspond to the nominal thickness of 1.5 nm. The density of protein was estimated to be $1.3 \pm 0.1$ g cm$^{-3}$.[32] The average frequency decrease of $340 \pm 86$ Hz for each Hb adsorption layer would then correspond to the nominal thickness of 8.9 nm, nearly twice as large as the Hb dimensions of $5.0 \times 5.5 \times 6.5$ nm.[33] Considering the experimental error and uncertainties in the estimation of film density and electrode area, the calculated thickness of the adsorption layers for both Dex and Hb is just a rough estimate.[3a]

LBL {Dex/protein(pH 5.0)}$_n$ films were also assembled on the PG electrode surface. After being abraded, the surface of basal plane PG became rough and the "edge" surface of PG was uncovered, which was negatively charged by virtue of the surface oxygen functionalities and had a partly hydrophobic character.[34] Thus, positively charged PEI was strongly adsorbed on the PG surface by both electrostatic and hydrophobic interactions and acted as the precursor layer. The following assembly of {Dex/protein(pH 5.0)}$_n$ films on PG/PEI surface was monitored by CV. Taking Mb as an example, after each adsorption cycle creating a new Dex/Mb bilayer, the electrode was washed with pure water and then transferred to a pH 7.0 buffer solution containing no Mb. A pair of well-defined, nearly reversible CV peaks was observed at about −0.35 V vs SCE (Figure 3), characteristic of the Mb heme Fe(III)/Fe(II) redox couple. The reduction and oxidation peak currents grew with the number of Dex/Mb bilayers ($n$) until $n = 6$. At $n > 6$, no further increase in the peak currents was observed, indicating that Mb in the seventh and following bilayers is not addressable electrochemically.

CVs of {Dex/protein(pH 5.0)}$_6$ films showed symmetric peak shapes and nearly equal heights of their reduction and oxidation

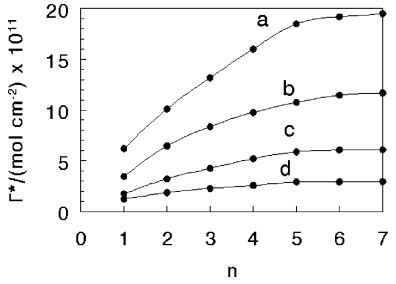


**Figure 4.** Influence of number of bilayers (*n*) on surface concentration of electroactive protein (Γ*) estimated by integration of CV reduction peak at 0.2 V $s^{-1}$ in pH 7.0 buffers for (a) {Dex/Mb(pH 5.0)}$_n$, (b) {Dex/Mb(pH 9.0)}$_n$, (c) {Dex/Hb(pH 5.0)}$_n$, and (d) {Dex/Hb(pH 9.0)}$_n$ films.

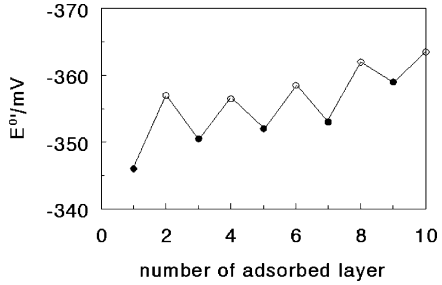


**Figure 5.** Effect of number of adsorbed layers on apparent formal potential ($E^{\circ\prime}$) estimated by CV at 0.2 V $s^{-1}$ in pH 7.0 buffers for {Dex/Mb(pH 5.0)}$_n$ films: (●) Mb on the outermost layer; (○) Dex on the outermost layer.

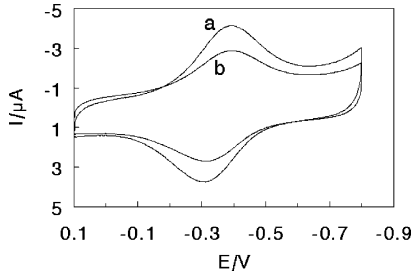


**Figure 6.** Cyclic voltammograms at 0.2 V $s^{-1}$ in pH 7.0 buffers for (a) {Dex/Mb(pH 5.0)}$_6$ and (b) {Dex/Mb(pH 9.0)}$_6$ films.

peaks. The heights of the reduction peaks were linearly proportional to scan rates from 0.05 to 5 V $s^{-1}$. These results are characteristic of diffusionless, surface-confined, or thin-layer electrochemistry,[35] suggesting that all electroactive heme Fe(III) of protein in the films is converted to heme Fe(II) on the forward cathodic scan, while on the reverse anodic scan all heme Fe(II) produced at electrodes is transformed back to heme Fe(III). In this case, integration of CV reduction peak that gives the charge (*Q*) value can be used to estimate the surface concentration of electroactive protein (Γ*, mol $cm^{-2}$) in the films with Faraday's law.[35] Compared with the UV−vis spectroscopic and QCM experiments (Figures 1 and 2) in which the growth of Dex/protein bilayer was essentially regular and uniform, the Γ* value of {Dex/protein(pH 5.0)}$_n$ films increased nonlinearly with *n* up to 6, and then reached a plateau and did not increase any more (Figure 4). Assuming the amount of adsorbed proteins in the first bilayer closest to the PG electrode surface is 100% electroactive, as observed in the previous works,[18] the fraction of electroactive proteins among the total adsorbed proteins in each bilayer could be estimated. The fraction decreased with *n* when $n < 7$. After *n* became larger than 7, the proteins in the films displayed hardly even any electroactivity, suggesting that the distance between the proteins and electrode surface is crucial for direct electron transfer.

In the assembly of LBL {Dex/protein(pH 5.0)}$_n$ films, a systematic shift of the peak potentials with the charge excess of the outermost layer was observed. For example, both reduction and oxidation peak potentials of {Dex/Mb(pH 5.0)}$_n$ films with the positively charged Mb as the outermost layer showed a positive shift compared with those of corresponding {Dex/Mb(pH 5.0)}$_n$Dex films with the negatively charged Dex as the outermost layer. Thus, the apparent formal potential, $E^{\circ\prime}$, estimated as a midpoint between reduction and oxidation peak potentials, switched systematically between about −0.36 and −0.34 V when the outermost layer switched between Dex and Mb in the LBL assembly (Figure 5). This result confirms the successful assembly of LBL films again and indicates the effect of the outermost charged region of the films on the Donnan potential ($\Delta\phi_D$).[36,37] The apparent formal potential of modified electrodes can be expressed as $E^{\circ\prime} = E^{\circ} + \Delta\phi_D$, where $E^{\circ}$ is the formal potential of the redox couple in the absence of an electrostatic work term due to the charged films.[37] Opposite charges on the outermost layer of the LBL films caused the distinct shift of the Donnan potential, and then induced the systematic change of $E^{\circ\prime}$ values, although the shift was only a few tens of millivolts. The $E^{\circ\prime}$ value showed a small shift to a more negative direction for the films with either Mb or Dex as the outermost layer when the number of adsorbed layers became larger than 8 (Figure 5), but the reason is not clear yet.

**3.2. Layer-by-Layer Assembly of Dex with Similarly Charged Proteins.** Both Hb and Mb have net negative charges on their surface at pH 9.0, while Dex in solution is always negatively charged independent of pH. Similarly charged Dex and proteins were also successfully assembled layer by layer on QCM Au/MPS/PEI and PG/PEI surface, designated as {Dex/protein(pH 9.0)}$_n$. QCM was used to monitor the growth of LBL {Dex/protein(pH 9.0)}$_n$ films. Taking {Dex/Hb(pH 9.0)}$_n$ films as an example, QCM results showed a roughly linear decrease of frequency with the adsorption step (Figure 2b). The frequency decrease for each Dex and Hb adsorption layer was 25 ± 13 and 185 ± 59 Hz, respectively. As expected, the adsorption amount of Hb and Dex in each bilayer for {Dex/Hb(pH 9.0)}$_n$ films was much smaller than that for {Dex/Hb(pH 5.0)}$_n$ films, respectively. The nominal thickness of 4.8 nm of Hb layer assembled at pH 9.0 was about half of a Hb layer assembled at pH 5.0 (8.9 nm), suggesting the formation of Hb monolayer at pH 9.0.

The LBL {Dex/protein(pH 9.0)}$_n$ films also showed a pair of reduction−oxidation peaks at about −0.35 V vs SCE for heme Fe(III)/Fe(II) redox couples, which grew with the number of bilayers when $n < 7$, while the peak height was much smaller than that of {Dex/protein(pH 5.0)}$_n$ films with the same *n* (Figure 6). The surface concentrations of electroactive proteins (Γ*) for {Dex/protein(pH 9.0)}$_n$ films were also smaller than those for the corresponding {Dex/protein(pH 5.0)}$_n$ films, but displayed a similar nonlinear growth trend with *n* up to 6 (Figure 4). The fraction of electroactive proteins among the total adsorbed proteins in each bilayer decreased with *n* when $n < 7$, also similar to the {Dex/protein(pH 5.0)}$_n$ films. The electrochemical parameters of LBL {Dex/protein}$_6$ films modified on PG electrodes are summarized in Table 1 for comparison.

At pH 9.0, while both Hb and Mb have net negative surface charges, they have considerable amounts of positively charged groups on their surface. Thus, the localized electrostatic attraction between negatively charged Dex and positively charged groups on the protein surface may overcome the repulsive interaction between Dex and proteins and enable the LBL

**TABLE 1: Electrochemical Parameters for LBL {Dex/Protein}$_6$ Films under Different Conditions**[a]

| protein | mol wt | isoelectric point | pH used | $E^{\circ\prime}$/V | $I_{pc}/\mu$A | $E_{pc}$/V | $I_{pa}/\mu$A | $E_{pa}$/V | $\Gamma^*$/(mol cm$^{-2}$) |
|---|---|---|---|---|---|---|---|---|---|
| Hb | 66 000 | 7.0−7.4 | 5.0 | −0.364 | −3.42 | −0.412 | 3.26 | −0.316 | $6.1 \times 10^{-11}$ |
| | | | 9.0 | −0.354 | −1.62 | −0.394 | 1.62 | −0.313 | $2.5 \times 10^{-11}$ |
| Mb | 17 800 | 6.8−7.0 | 5.0 | −0.355 | −2.68 | −0.398 | 2.60 | −0.311 | $2.0 \times 10^{-10}$ |
| | | | 9.0 | −0.349 | −1.73 | −0.381 | 1.72 | −0.317 | $1.1 \times 10^{-10}$ |

[a] Data from CVs at 0.2 V s$^{-1}$ in pH 7.0 buffers. *E* vs SCE.

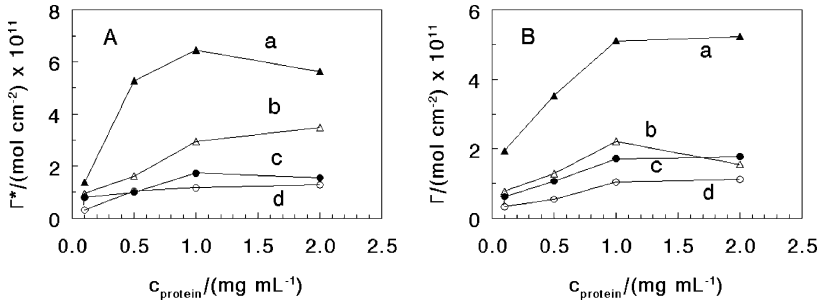


**Figure 7.** Influence of protein concentration ($c_{protein}$) on (A) surface concentration of electroactive protein ($\Gamma^*$) estimated by CV at 0.2 V s$^{-1}$ in pH 7.0 buffers and (B) surface concentration of protein ($\Gamma$) measured by QCM for (a) {PEI/Dex}$_2$/Mb(pH 5.0), (b) {PEI/Dex}$_2$/Mb(pH 9.0), (c) {PEI/Dex}$_2$/Hb(pH 5.0), and (d) {PEI/Dex}$_2$/Hb(pH 9.0) films.

assembly to be realized. However, this localized attraction would be weakened by the repulsion for {Dex/protein(pH 9.0)}$_n$ films if compared with the regular assembly of {Dex/protein(pH 5.0)}$_n$ films, resulting in a smaller amount of proteins absorbed.

To further investigate the properties of interaction between Dex and proteins with different net surface charges, the influence of protein concentration, the ionic strength, and the applied electric field on adsorption of the proteins on the Dex surface was studied in detail. In these studies, two PEI/Dex bilayers were first assembled on PG or Au/MPS surface as precursor layers. The two-bilayer precursor of {PEI/Dex}$_2$ was used here to make the electrode surface more uniform and the following adsorption of proteins more reproducible from one preparation to another.[38] The heme proteins under different conditions were then adsorbed onto PG/{PEI/Dex}$_2$ or Au/MPS/{PEI/Dex}$_2$ surface. CV and QCM were used to characterize the protein adsorption.

**3.3. Influence of Protein Concentration.** Hb or Mb in their solutions at pH 5.0 or 9.0 with different concentrations and constant ionic strength (0.3 M NaCl) was assembled on PG/{PEI/Dex}$_2$ surface by adsorption. The {PEI/Dex}$_2$/protein films were then transferred to blank buffers at pH 7.0, and CVs were conducted. In all cases, the {PEI/Dex}$_2$/protein films showed a heme Fe(III)/Fe(II) peak pair at about −0.35 V vs SCE, and as expected, the CV reduction peak currents showed a sequence of {PEI/Dex}$_2$/protein(pH 5.0) > {PEI/Dex}$_2$/protein(pH 9.0) for both Hb and Mb. Figure 7A shows the effect of protein concentration ($c_{protein}$) on the surface concentration of electroactive protein ($\Gamma^*$) of {PEI/Dex}$_2$/protein films assembled under different pH conditions. In all cases, the $\Gamma^*$ values increased with the protein concentration up to about 1 mg mL$^{-1}$, and then tended to level off or even slowly decrease. To further investigate the influence of protein concentration, QCM was used and the surface concentration of protein ($\Gamma$, mol cm$^{-2}$) was estimated at different $c_{protein}$ values by taking into account the adsorption mass of protein, the Au electrode area (0.196 cm$^2$), and the molecular weight of protein (Figure 7B). Generally, the surface concentration of protein measured by QCM ($\Gamma$) was smaller than that estimated by CV ($\Gamma^*$) for the same protein and under the same conditions, although the difference was not large. This difference is probably caused by the different roughness of PG and Au electrodes. In the estimation of the surface concentration of protein, the geometric area of the electrodes was used. However, since the roughness of PG was much larger than that of Au, the actual area of PG was greater. The difference of roughness between two electrodes may become smaller after the adsorption of {PEI/Dex}$_2$ precursor layers on the electrode surface but still exist. In plot of $\Gamma - c_{protein}$, QCM results showed a trend very similar to that of CV (Figure 7), suggesting that a protein concentration greater than 1 mg mL$^{-1}$ in adsorbate solutions would not increase the amount of adsorbed proteins at either pH 5.0 or 9.0. A concentration of 1 mg mL$^{-1}$ was thus chosen as the optimal protein concentration in adsorbate solutions to construct {PEI/Dex}$_2$/protein films in the following studies.

**3.4. Effect of Ionic Strength.** The amount of adsorbed proteins was significantly affected by the ionic strength (or NaCl concentration in this study) in protein adsorbate solution for {PEI/Dex}$_2$/protein films (Figure 8). For different proteins and at different assembly pH values, the $\Gamma^* - c_{NaCl}$ curves measured by CV were different, but all of them showed a similar peaklike curve shape and had nearly the same peak position. $\Gamma^*$ values increased with the ionic strength at low NaCl concentration and decreased with the ionic strength at high NaCl concentration, passing through a maximum point at about 0.3 M NaCl in the course (Figure 8A). QCM was also used to investigate the influence of ionic strength, and the results were essentially consistent with those of CV (Figure 8B). Both electrostatic attraction and repulsion existed in the adsorption of protein on {PEI/Dex}$_2$ surface, and the ionic strength had different influences on these two different kinds of electrostatic interactions. The appearance of a maximum in both $\Gamma^* - c_{NaCl}$ and $\Gamma - c_{NaCl}$ plots was an indication of counterbalance between two types of interactions with opposite directions, suggesting that the main driving force for the assembly of proteins on {PEI/Dex}$_2$ surface would be of electrostatic origin independent of the pH in protein adsorbate solution.[39]

**3.5. Protein Adsorption under an Applied Electric Field.** Recently, the electric field directed LBL assembly (EFDLA) approach was employed to realize site-selective deposition of enzyme/polyelectrolyte multilayer films on indium tin oxide (ITO) electrodes.[40] The applied electric field may greatly promote or inhibit the LBL assembly of oppositely charged species dependent on the direction of the electric field. The adsorption of proteins on {PEI/Dex}$_2$ surface under different electric fields was investigated here using the three-electrode

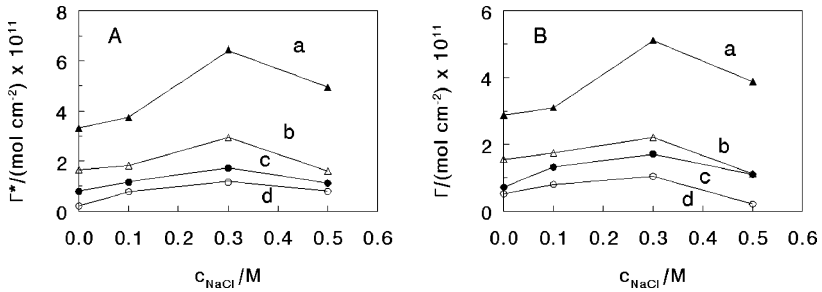


**Figure 8.** Effect of NaCl concentration ($c_{NaCl}$) on (A) surface concentration of electroactive protein ($\Gamma^*$) estimated by CV at 0.2 V $s^{-1}$ in pH 7.0 buffers and (B) surface concentration of protein ($\Gamma$) measured by QCM for (a) $\{PEI/Dex\}_2$/Mb(pH 5.0), (b) $\{PEI/Dex\}_2$/Mb(pH 9.0), (c) $\{PEI/Dex\}_2$/Hb(pH 5.0), and (d) $\{PEI/Dex\}_2$/Hb(pH 9.0) films.

**TABLE 2: Ex Situ QCM Results for Each Protein Layer Adsorbed on Au/MPS/$\{PEI/Dex\}_2$ Surface at Different pH Values and Different Potentials of the Applied Electric Field**

| applied | Hb (pH 5.0) | | Hb (pH 9.0) | | Mb (pH 5.0) | | Mb (pH 9.0) | |
|---|---|---|---|---|---|---|---|---|
| *E*/V vs SCE | Δ*M*/ng | *d*[a]/nm | Δ*M*/ng | *d*[a]/nm | Δ*M*/ng | *d*[a]/nm | Δ*M*/ng | *d*[a]/nm |
| −0.1 | 360.45 | 14.0 | 112.05 | 4.3 | 311.85 | 12.0 | 116.1 | 4.5 |
| OCP[b] | 283.5 | 11.0 | 184.95 | 7.1 | 251.1 | 9.7 | 148.5 | 5.7 |
| +0.5 | 179.55 | 7.0 | 145.8 | 5.6 | 149.85 | 5.8 | 136.35 | 5.3 |

[a] *d*, nominal thickness estimated by QCM. [b] OCP, open circuit potential.

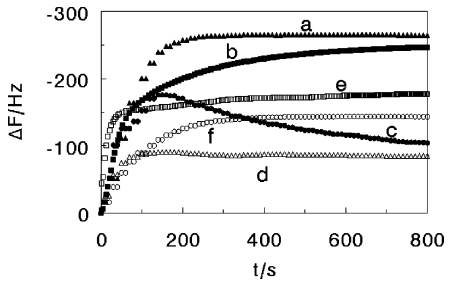


**Figure 9.** In situ QCM frequency shift with adsorption time for Au/MPS/$\{PEI/Dex\}_2$ films in Mb adsorbate solutions at different pH values and different potentials of the applied electric field: (a, ▲) pH 5.0, −0.1 V; (b, ■) pH 5.0, OCP; (c, ●) pH 5.0, +0.5 V; (d, △) pH 9.0, −0.1 V; (e, □) pH 9.0, OCP; (f, ○) pH 9.0, +0.5 V.

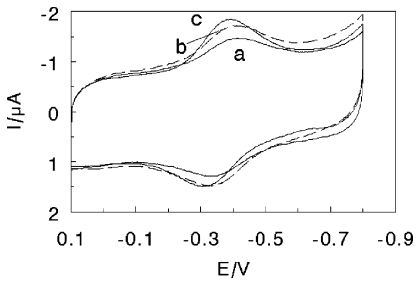


**Figure 10.** Cyclic voltammograms for $\{PEI/Dex\}_2$/Hb(pH 5.0) films at scan rate of 0.2 V $s^{-1}$ in pH 7.0 buffer solutions with different potentials of the applied electric field: (a) +0.5 V; (b) OCP; (c) −0.1 V.

cell system with SCE as the reference electrode. The preliminary experiments showed that the appropriate potential range applied to the $\{PEI/Dex\}_2$/protein system would be between +0.6 and −0.2 V vs SCE. Potential higher than 0.6 V or lower than −0.2 V would cause an electron transfer reaction of solvent or proteins at the electrodes, and should be avoided. The open circuit potential (OCP) of the studied system was usually at about 0.1 V, within the appropriate applied potential range. Thus, +0.5 V was chosen as a high voltage or positive potential, and −0.1 V was selected as a low voltage or negative potential of the applied electric field on working electrodes. The voltage-dependent adsorption of proteins on Au/MPS/$\{PEI/Dex\}_2$ surface was investigated and characterized by in situ QCM. For example, Figure 9 presents the frequency shift (Δ*F*) with adsorption time measured by in situ QCM for Mb at different pH values and various applied potentials, in which the surface of gold resonator electrodes was modified with MPS/$\{PEI/Dex\}_2$ films. The results of OCP here represented the normal adsorption of Mb on the surface without applying any voltage. At pH 5.0, Mb in solution had net positive surface charges. Thus, the negative potential of −0.1 V applied to the electrode would be favorable to the adsorption of positively charged Mb from its solution on $\{PEI/Dex\}_2$ surface. On the contrary, the positive potential of +0.5 V would decrease the amount of adsorbed Mb from its pH 5.0 solution. The adsorption amount of Mb thus showed a potential sequence of −0.1 V > OCP > +0.5 V at the steady state. Moreover, curve c (pH 5.0, +0.5 V) in Figure 9 showed a maximum peak and reached the steady state in about 800 s, which was different from the other curves. On the other hand, for negatively charged Mb in pH 9.0 solution, the positive potential of +0.5 V would be more favorable to Mb adsorption than the negative potential of −0.1 V, which was also confirmed by in situ QCM experiments at the steady state (Figure 9). However, in pH 9.0 solution, the adsorption amount of Mb at OCP was not only larger than that at −0.1 V but also larger than that at +0.5 V at the steady state, and curve e (pH 9.0, OCP) in Figure 9 showed a larger decreasing rate than the others. Moreover, the ex situ QCM results for the protein layers adsorbed on $\{PEI/Dex\}_2$ surface on one side of the QCM gold resonator under different conditions were also obtained after the films reached the adsorption equilibrium and were dried in a nitrogen stream (Table 2). The adsorption amount of Hb or Mb and the nominal thickness of the protein layer estimated by ex situ QCM under different conditions are qualitatively consistent with the in situ QCM results.

The adsorption of heme proteins at the applied electric field was also realized on PG/$\{PEI/Dex\}_2$ electrode surface. The CV of $\{PEI/Dex\}_2$/protein films assembled at different pH values and different potentials of the applied electric field all showed a pair of chemically reversible reduction−oxidation peaks at about −0.35 V in pH 7.0 buffers. The change of surface concentration of electroactive proteins ($\Gamma^*$) with the applied potential also displayed behavior similar to that of the QCM results (for example, Figure 10). This confirms that while the applied electric field in the range of −0.1 to +0.5 V has different

effects on the adsorption amount of proteins with different net surface charges, it has little effect on the electroactivity of heme proteins. When the applied electric field altered from +0.5 V to −0.1 V, the redox peak current of $\{PEI/Dex\}_2$/Hb(pH 5.0) films increased, accompanied by the gradual shift of the reduction peak position to a lower overpotential direction (Figure 10), indicating that the negative potential of −0.1 V would be more favorable to both adsorption and reduction of positively charged Hb than the positive potential of +0.5 V.

## 4. Discussion

**4.1. Driving Forces for the Assembly.** Our above experimental results indicate that Coulombic attraction between oppositely charged Dex and heme proteins plays a key role in the assembly of LBL $\{Dex/protein(pH\ 5.0)\}_n$ films (Figures 1−3). When the proteins have positive net surface charges at pH 5.0, the adsorption amount on the oppositely charged Dex surface is much greater compared to the proteins with net negative charges (Figures 4 and 6−8, Table 1). Therefore, to obtain the greatest or optimum adsorption amount of the protein on the surface of polyelectrolyte, the overall surface charges of the protein and polyelectrolyte must be opposed. This regular growth mode was thus used in most of the studies on protein/polyion LBL assembly.[3,8,9] However, when Hb or Mb carried the net negative surface charges at pH 9.0, the adsorption of proteins on the similar charged Dex surface was also observed (Figures 4 and 6−8, Table 1). The adsorption amount of proteins was smaller than that with regular growth mode but still quite significant. These results seem difficult to explain by simple electrostatic interaction, and suggest a more complicated situation or character of the driving forces in protein LBL assembly.

The experimental results that LBL films of proteins and polyelectrolyte with similar net surface charges could be successfully constructed were also reported previously.[14−17,41] For example, Schenkman et al.[17] found that the essentially anionic cytochrome P450 (Cyt P450) enzymes could be adsorbed on negatively charged poly(styrenesulfonate) (PSS) surface, although the adsorption amount was smaller than that on positively charged PEI surface. This adsorption was attributed to electrostatic attraction between PSS and some positively charged location on the protein surface, although the overall net surface charge of the protein was negative. Cyt P450 enzymes had "charge patches" of different signs on different sides, which imparted a sidedness to these protein molecules. We thus also consider the influence of localized surface charges of Mb and Hb in our present work. At appropriate pH, the arginine (Arg), lysine (Lys), and histidine (His) residues on the protein surface may have positive charges, while the aspartic acid (Asp) and glutamic acid (Glu) residues may have negative charges. The corresponding $pK_a$ values of these residues for horse heart Mb and bovine Hb are known in the literature.[26,42−45] Thus, the number of charged amino acid groups on Hb and Mb surface at different pH values can be estimated. Taking Mb as an example, there are 19 Lys ($pK_a$ = 10−12) and 2 Arg ($pK_a$ = 12−13) residues on the Mb surface, and the total number of positively charged surface Lys and Arg residues is 21 at both pH 5.0 and 9.0. Thus, at pH 9.0, while the net surface charge of Mb is negative, there are still a considerable number of positively charged groups on the Mb surface. Some of these positively charged surface groups may interact with the flexible long-chain polyanionic Dex by electrostatic attraction. This localized electrostatic interaction may be the main driving force for the LBL assembly of $\{Dex/Mb(pH\ 9.0)\}_n$ films. This is similar to what has been observed with Cyt P450 enzymes on polyion surfaces,[17] but in that case different sides of the enzyme retained localized charged patches of opposite sign. Mb does not seem to have such charge patches on its surface, having a more even distribution of surface charges. Yet the localized electrostatic attractions of the Lys and Arg groups of the proteins with the oppositely charged Dex may be strong enough for the proteins to participate in film assembly even at pH 9.0. On the other hand, the "structure" of Mb at pH 5.0 seems to differ from that at pH 9.0. Every Mb molecule has 6 His residues on its surface.[46] These surface His residues with $pK_a$ of 6−7 will be protonated at pH 5.0 and noncharged at pH 9.0. Thus, at pH 5.0, the positively charged groups on the Mb molecule surface will increase and greater amounts of Mb will be adsorbed on the Dex surface with stronger electrostatic attractions between them compared with those at pH 9.0.

For the adsorption mechanism of the protein at pH 9.0 on $\{PEI/Dex\}_2$ surface, there exists another possibility. Although the outer layer of the $\{PEI/Dex\}_2$ films mainly consists of polyanionic Dex, some parts of polycationic PEI underneath may penetrate or emerge from the Dex layer. The interaction between the positively charged PEI groups and the negatively charged proteins at pH 9.0 would also benefit the adsorption of proteins.

**4.2. Influencing Factors for the Assembly.** The ionic strength in protein adsorbate solution has a significant influence on the amount of proteins adsorbed on $\{PEI/Dex\}_2$ surface (Figure 8). Taking $\{PEI/Dex\}_2$/Mb(pH 5.0) as an example, when the concentration of NaCl was below 0.3 M, the surface concentration of electroactive Mb ($\Gamma^*$) increased with the ionic strength, while at NaCl concentration greater than 0.3 M the $\Gamma^*$ value gradually decreased with the ionic strength, having a maximum adsorption amount at 0.3 M NaCl (Figure 8A). The QCM experiment displayed a similar result (Figure 8B). This peaklike curve was also observed in other polyion/protein adsorption systems with the characteristic of electrostatic interactions.[14] There are two contrary or opposite forces in the adsorption of Mb on Dex surface: the attraction between positively charged Mb and polyanionic Dex, and repulsion between two individual Mb molecules with the same positive charges. Both interactions are of electrostatic origin and are thus affected by the salt concentration. In the high salt concentration range, the attractive interaction is considered to be the predominant force. The increase of ionic strength would weaken the interactions between Mb and oppositely charged Dex because of the screening effect, leading to a decrease of the amount of adsorbed Mb. In the lower salt concentration range, on the other hand, the repulsive interaction between Mb molecules becomes the dominant force in Mb adsorption. The increase of ionic strength would reduce the repulsive interaction acting laterally between two individual Mb molecules, leading to a more compact arrangement of adsorbed Mb molecules, and thus resulting in an increase of the amount of adsorbed Mb. It could therefore be understandable that a maximum in the adsorbed amount was observed as a function of the ionic strength for the $\{PEI/Dex\}_2$/Mb(pH 5.0) system (Figure 8), which usually comes out when two antagonistic forces govern a physical process.

The peaklike curve of the adsorption amount of proteins vs ionic strength is also observed for $\{PEI/Dex\}_2$/protein(pH 9.0) system (Figure 8). As discussed above, the driving force for the adsorption of negatively charged protein at pH 9.0 on the like-charged $\{PEI/Dex\}_2$ surface is also of electrostatic origin. Thus, the adsorption amount of the proteins would be dependent on ionic strength and demonstrate behavior similar to that of

the {PEI/Dex}$_2$/protein(pH 5.0) system. Sometimes the adsorption amount of proteins at 0.5 M NaCl was even smaller than that at 0 M NaCl (Figure 8), indicating that the enhanced screening effect at such a high concentration of NaCl would greatly repress the adsorption of proteins on Dex.

The influence of an applied electric field on the amount of adsorbed heme proteins on {PEI/Dex}$_2$ surface was investigated by QCM and CV (Table 2, Figures 9 and 10). For positively charged proteins at pH 5.0, the low voltage or negative potential of −0.1 V would increase the amount of adsorbed proteins, compared with the high voltage or positive potential of +0.5 V. For negatively charged proteins at pH 9.0, the situation is reversed. However, in pH 9.0 solution, the adsorption amount of Mb at OCP was even larger than that at +0.5 V at the steady state. Proteins with a net negative charge have positive groups on their surface that allow localized binding of them with Dex. At positive potential of +0.5 V, this localized binding could be repressed and therefore an immobilization of Mb at OCP might be more favorable. Probably for the same reason, the adsorption rate of negatively charged Mb at OCP was more rapid than that at either −0.1 or +0.5 V, showing a larger decreasing rate in QCM frequency (Figure 9e). These results confirm that the interaction between the proteins and Dex is mainly of electrostatic origin regardless of the type of protein surface charges.

At pH 5.0, the nominal thickness of Hb estimated by QCM is in the range of 11.0−14.0 nm at the open circuit potential or negative potential of −0.1 V (Table 2). This thickness is about twice the dimensions of Hb (5.0 × 5.5 × 6.5 nm),[33] indicating that about two Hb monolayers are adsorbed on the oppositely charged Dex surface. Similarly, at pH 5.0, the nominal thickness of Mb is between 9.7 and 12.0 nm at OCP or −0.1 V (Table 2), suggesting that at least two Mb monolayers are adsorbed if considering its size (2.5 × 3.5 × 4.5 nm).[47] A possible explanation for this is that when the first monolayer of proteins is adsorbed on Dex surface, some of the flexible and long-chain Dex polyelectrolyte may emerge from the protein layer. The Dex may interact with the whole protein molecule in a kind of encapsulation process. It is known that, in solution, proteins form strong complexes with polyelectrolyte through a kind of encapsulation process.[48] Thus, once a first layer of protein molecules is adsorbed on Dex, some Dex may still be on top of the adsorbed protein monolayer, and new protein molecules from the solution may interact with these Dex polyions by attraction and adsorb on it, forming another protein monolayer. However, as the thickness of the protein layer increases further, fewer Dex polyelectrolytes can reach the outer part of the protein layer so that the adsorption process stops. While the experimental evidence for this explanation is absent now and further studies are needed, similar results and corresponding explanation are also reported in the literature.[14,16]

On the other hand, when the proteins carry the negative charges at pH 9.0, the maximum nominal thickness estimated by QCM is only about 7.1 nm for Hb and 5.7 nm for Mb (Table 2), much smaller than that at pH 5.0 and roughly equal to the monolayer dimensions of Hb and Mb, respectively. This is most probably because of the repulsive interaction between the proteins and Dex. While the localized electrostatic attraction between the positively charged groups on the protein surface and polyanionic Dex makes the proteins adsorb on Dex surface even at pH 9.0, the net negative surface charges of the proteins at this pH would make the repulsion between the proteins and Dex become stronger compared with that at pH 5.0, resulting in less adsorption of proteins.

## 5. Conclusion

The heme proteins (Hb or Mb) with either net positive charges or net negative charges on their surfaces at different pH values and negatively charged polyelectrolyte dextran sulfate were successfully assembled into layer-by-layer films on a variety of solid substrates. No matter the kind of overall charges of the proteins, the main driving force for the proteins to adsorb onto the Dex layer surface would be of electrostatic origin. There are considerable amounts of positively charged surface residues on the protein surface even when the overall charges of the protein are negative at pH higher than its isoelectric point. The flexible long chains of Dex with negative charges on its backbone would prefer to combine with these positively charged groups by Coulombic attraction. This localized electrostatic interaction is most probably the main driving force for the LBL assembly even when the proteins and Dex have the same net negative surface charges. The understanding of the essence of the adsorption process is of prime importance for the design of complex protein multilayer films with specific biological and/or catalytic activities.

**Acknowledgment.** The financial support from the National Natural Science Foundation of China (NSFC, 20275006, 29975003), and the State Key Laboratory of Electroanalytical Chemistry of Changchun Institute of Applied Chemistry, the Chinese Academy of Sciences, is greatly appreciated.

## References and Notes

(1) (a) Lvov, Y. In *Protein Architecture: Interfacing Molecular Assemblies and Immobilization Biotechnology*; Lvov, Y., Mohwald, H., Eds.; Marcel Dekker: New York, 2000; pp 125−167. (b) Lvov, Y. In *Nanostructured Materials, Micelles and Colloids*; Nalwa, R. W., Ed.; Handbook of Surfaces and Interfaces of Materials 3; Academic Press: San Diego, 2001; pp 170−189.

(2) (a) Rusling, J. F. In *Protein Architecture: Interfacing Molecular Assemblies and Immobilization Biotechnology*; Lvov, Y., Mohwald, H., Eds.; Marcel Dekker: New York, 2000; pp 337−354. (b) Rusling, J. F.; Zhang, Z. In *Biomolecules, Biointerfaces, and Applications*; Nalwa, R. W., Ed.; Handbook of Surfaces and Interfaces of Materials 5; Academic Press: San Diego, 2001; pp 33−71.

(3) (a) Lvov, Y.; Ariga, K.; Ichinose, I.; Kunitake, T. *J. Am. Chem. Soc*. **1995**, *117*, 6117. (b) Lvov, Y. M.; Lu, Z.; Schenkman, J. B.; Zu, X.; Rusling, J. F. *J. Am. Chem. Soc*. **1998**, *120*, 4073.

(4) (a) Kimizuka, N.; Tanaka, M.; Kunitake, T. *Chem. Lett*. **1999**, *12*, 1333. (b) Lvov, Y.; Munge, B.; Giraldo, O.; Ichinose, I.; Suib, S.; Rusling, J. F. *Langmuir* **2000**, *16*, 8850.

(5) Ariga, K.; Kunitake, T. In *Protein Architecture: Interfacing Molecular Assemblies and Immobilization Biotechnology*; Lvov, Y., Mohwald, H., Eds.; Marcel Dekker: New York, 2000; pp 169−192.

(6) For selected examples, see: (a) Hodak, J.; Etchenique, R.; Calvo, E. J.; Singhal, K.; Bartlett, P. N. *Langmuir* **1997**, *13*, 2708. (b) Zhang, X.; Sun, Y.; Shen, J. In *Protein Architecture: Interfacing Molecular Assemblies and Immobilization Biotechnology*; Lvov, Y., Mohwald, H., Eds.; Marcel Dekker: New York, 2000; pp 229−250. (c) Zhou, L.; Rusling, J. F. *Anal. Chem.* **2001**, *73*, 4780. (d) Mugweru, A.; Rusling, J. F. *Anal. Chem.* **2002**, *74*, 4044. (e) Dennany, L.; Forster, R. J.; Rusling, J. F. *J. Am. Chem. Soc.* **2003**, *125*, 5213. (f) Zhou, L.; Yang, J.; Estavillo, C.; Stuart, J. D.; Schenkman, J. B.; Rusling, J. F. *J. Am. Chem. Soc.* **2003**, *125*, 1431.

(7) Lambert, G.; Fattal, E.; Couvreur, P. *Adv. Drug Delivery Rev.* **2001**, *47*, 99.

(8) (a) Ma, H.; Hu, N.; Rusling, J. F. *Langmuir* **2000**, *16*, 4969. (b) He, P.; Hu, N.; Zhou, G. *Biomacromolecules* **2002**, *3*, 139. (c) Zhou, Y.; Li, Z.; Hu, N.; Zeng, Y.; Rusling, J. F. *Langmuir* **2002**, *18*, 8573. (d) Li, Z.; Hu, N. *J. Electroanal. Chem.* **2003**, *558*, 155. (e) Wang, L.; Hu, N. *Bioelectrochemistry* **2001**, *53*, 205.

(9) (a) Yu, X.; Sotzing, G. A.; Papadimitrakopoulos, F.; Rusling, J. F. *Anal. Chem*. **2003**, *75*, 4565. (b) Munge, B.; Estavillo, C.; Schenkman, J. B.; Rusling, J. F. *ChemBioChem* **2003**, *4*, 101. (c) Jin, Y.; Shao, Y.; Dong, S. *Langmuir* **2003**, *19*, 4771. (d) Zhao, J.; Liu, B.; Zou, Y.; Chen, X.; Kong, J. *Electrochim. Acta* **2002**, *47*, 2013. (e) Shang, L.; Liu, X.; Zhong, J.; Fan, C.; Suzuki, I.; Li, G. *Chem. Lett*. **2003**, *32*, 296.

(10) Chaplin, M. F.; Bucke, C. *Enzyme Technology*; Cambridge University Press: Cambridge, UK, 1990.

(11) Armstrong, F. A.; Wilson, G. S. *Electrochim. Acta* **2000**, *45*, 2623.

(12) (a) Rusling, J. F. *Acc. Chem. Res.* **1998**, *31*, 363. (b) Hu, N. *Pure Appl. Chem.* **2001**, *73*, 1979.

(13) Decher, G. *Science* **1997**, *227*, 1232.

(14) Ladam, G.; Gergely, C.; Senger, B.; Decher, G.; Voegel, J.-C.; Schaaf, P.; Cuisiner, F. J. G. *Biomacromolecules* **2000**, *1*, 674.

(15) Ladam, G.; Schaaf, P.; Cuisinier, F. J. G.; Decher, G.; Voegel, J.-C. *Langumir* **2001**, *17*, 878.

(16) Ladam, G.; Schaaf, P.; Decher, G.; Voegel, J.-C.; Cuisinier, F. J. G. *Biomol. Eng.* **2002**, *19*, 273.

(17) Schenkman, J. B.; Jansson, I.; Lvov, Y. M.; Rusling, J. F.; Boussaad, S.; Tao, N. J. *Arch. Biochem. Biophys*. **2001**, *385*, 78.

(18) He, P.; Hu, N.; Rusling, J. F. *Langmuir* **2004**, *20*, 722.

(19) Hammond, P. T. *Curr. Opin. Colloid Interface Sci.* **2000**, *4*, 430.

(20) Stockton, W. B.; Rubner, M. F. *Macromolecules* **1997**, *30*, 2717.

(21) Raposo, M.; Oliverira, O. N., Jr. *Langmuir* **2002**, *18*, 6866.

(22) Whateley, T. L. *Macroencapsulation of Drugs*; Harwood Academic Publishers: Amsterdam, 1992.

(23) Serizawa, T.; Yamaguchi, M.; Matsuyama, T.; Akashi, M. *Biomacromolecules* **2000**, *1*, 306.

(24) Qiu, X.; Leporatti, S.; Donath, D.; Mohwald, H. *Langmuir* **2001**, *17*, 5375.

(25) Serizawa, T.; Yamaguchi, M.; Akashi, M. *Macromolecules* **2002**, *35*, 8656.

(26) Matthew, J. B.; Hanania, G. I. H.; Gurd, F. R. N. *Biochemistry* **1979**, *18*, 1919.

(27) Yang, L.; Lee, C. S.; Hofstadler, S. A.; Pasa-Tolic, L.; Smith, R. D. *Anal. Chem*. **1998**, *70*, 3235.

(28) Bellelli, A.; Antonini, G.; Brunori, M.; Springer, B. A.; Sligar, S. J. *J. Biol. Chem*. **1990**, *265*, 18898.

(29) Theorell, H.; Ehrenberg, A. *Acta Chem. Scand.* **1951**, *5*, 823.

(30) Sauerbrey, G. *Z. Phys.* **1959**, *155*, 206.

(31) *Polymer Handbook*; Brandrup, J., Immergut, E., Eds.; Wiley-Interscince: New York, 1975; Part 5.

(32) *Protein Structure, a Practical Approach*; Creighton, T. E., Ed.; IRL Press: New York, 1990; p 43.

(33) Perutz, M.; Muirhead, H.; Cox, J.; Goaman, L.; Mathews, L.; McGandy, E.; Webb, L. *Nature* **1968**, *219*, 29.

(34) Hill, H. A. O. *Pure Appl. Chem.* **1987**, *59*, 743.

(35) Murray, R. W. In *Electroanalytical Chemistry*; Bard, A. J., Ed.; Dekker: New York, 1984; Vol. 13, p 191.

(36) Hodak, J.; Etchenique, R.; Calvo, E. J.; Singhal, K.; Bartlett, P. N. *Langmuir* **1997**, *13*, 2716.

(37) Calvo, E. J.; Wolodiuk, A. *J. Am. Chem. Soc.* **2002**, *124*, 8490.

(38) Ladam, G.; Schaad, P.; Voegel, J. C.; Schaaf, P.; Decher, G.; Cuidinier, F. *Langmuir* **2000**, *16*, 1249.

(39) Muller, M.; Rieser, T.; Dubin, P. L.; Lunkwitz, K. *Macromol. Rapid Commun*. **2001**, *22*, 390.

(40) (a) Shi, L.; Sun, J.; Liu, J.; Shen, J.; Gao, M. *Chem. Lett.* **2002**, 1168. (b) Shi, L.; Lu, Y.; Sun, J.; Zhang, J.; Sun, C.; Liu, J.; Shen, J. *Biomacromolecules* **2003**, *4*, 1161.

(41) Topoglidis, E.; Campbell, C. J.; Cass, A. E. G.; Durrant, J. R. *Langmuir* **2001**, *17*, 7899.

(42) Yang, A.-S.; Honig, B. *J. Mol. Biol.* **1994**, *237*, 602.

(43) Shire, S. J.; Hanania, I. H.; Gurd, F. R. N. *Biochemistry* **1974**, *13*, 2967.

(44) Friend, S. H.; Gurd, F. R. N. *Biochemistry* **1979**, *18*, 4612.

(45) Bashford, D.; Case, D. A.; Dalvit, C.; Tennant, L.; Wright, P. E. *Biochemistry* **1993**, *32*, 8045.

(46) Stigter, D.; Alonso, D. O. V.; Dill, K. A. *Proc. Natl. Acad. Sci. U.S.A.* **1991**, *88*, 4176.

(47) Kendrew, J.; Phillips, D.; Stone, V. *Nature* **1960**, *185*, 422.

(48) Takahashi, D.; Kubota, Y.; Kokai, K.; Izumi, T.; Hirata, M.; Kokufuta, E. *Langmuir* **2000**, *16*, 3133.